

Characterization of neutral density profile in a wide range of pressure of cylindrical pulsed gas jets

V. Malka,^{a)} C. Coulaud, J. P. Geindre, and V. Lopez

LULI, CNRS-CEA, Ecole Polytechnique-Université Pierre et Marie Curie, 91128 Palaiseau Cedex, France

Z. Najmudin

Imperial College, Blackett Laboratory, Prince Consort Road, London SW7 2AZ, United Kingdom

D. Neely

Rutherford Appleton Laboratory, Chilton, Didcot, Oxon OX11 0QX, United Kingdom

F. Amiranoff

LULI, CNRS-CEA, Ecole Polytechnique-Université Pierre et Marie Curie, 91128 Palaiseau Cedex, France

(Received 14 October 1999; accepted for publication 16 February 2000)

The neutral density profile of cylindrical gas jets is measured with a Mach-Zehnder interferometer under a wide range of backing pressures. The sensitivity of this diagnostic together with the mathematical treatment of the data allows us to measure neutral densities for argon gas as low as 10^{17} cm^{-3} for a 5 mm diam gas jet. © 2000 American Institute of Physics.

[S0034-6748(00)03906-X]

I. INTRODUCTION

The use of gas jets to generate a suitable density interaction medium is important in the field of laser plasma interactions in areas such as laser particle acceleration (LPA),^{1,2} inertial confinement fusion (ICF),^{3,4} x-ray lasers,⁵ and high harmonic generation.⁶ For example, in the context of ICF work, focusing a nanosecond laser pulse with a random phase plate (in order to get a large focal spot) a long laser pulse onto the edge of a gas jet provides large scale length (few mm), uniform, quasistatic and reproducible plasmas. Focusing a laser pulse with a spherical or an axicon lens onto the edge of the gas jet can generate a preformed channel.⁷⁻⁹ This plasma channel can be used to guide a short and intense laser pulse over a much longer distance than the diffraction limited one. This self-guiding has applications for x-ray laser research or energetic (MeV) electron generation. Controlling the gas flow is essential to provide the desired interaction density. For example, using a sonic or a supersonic gas flow

will provide a uniform or a parabolic neutral density profile. Changing the gas pressure will change the initial neutral density. Using a combination of gases will give a plasma with a mixture of different ions species. Changing the nozzle diameter could change the plasma length. Compared to the thin exploding foil techniques, the use of a gas jet presents some interesting advantages. In the thin foil technique one focuses a laser beam onto the foil. The thin foil is heated and explodes symmetrically, and the density decreases rapidly from the solid density to the subcritical desired density, giving a parabolic density profile. When creating a plasma using gas jets, the desired density is reached by choosing the initial gas pressure. This crucial point gives the advantage of creating large scale plasmas using moderate laser energy and having a quasistatic plasma with a controlled density profile. Finally, the use of a gas jet will give us the opportunity to create plasmas with different characteristics than those obtained with conventional targets. Previous measurements were car-

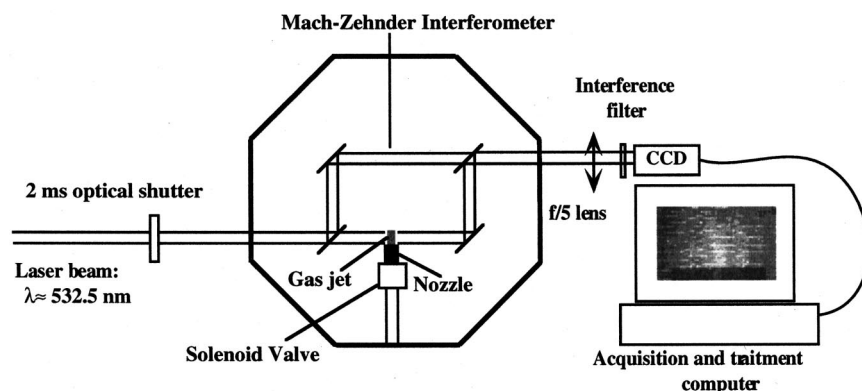


FIG. 1. Experimental setup.

^{a)}Electronic mail: victor@greco2.polytechnique.fr

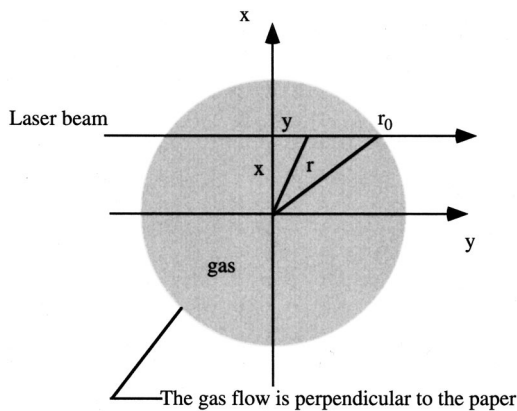


FIG. 2. Schematic of the Abel transformation. The gas flow is perpendicular to the page.

ried out using an interferometer with a sonic jet^{10,11} expanding in vacuum and with a supersonic jet expanding in air.¹²

In this article we report on an experiment performed using axisymmetrical nozzles. Both supersonic and sonic gas flow measurements are detailed here. The gas flow is measured by interferometric measurements over a wide range of pressure. The phase shift induced by the gas jet is experimentally detected by measuring the fringe displacement from their unperturbed position obtained in the vacuum. A comparison between interferograms, obtained with and without gas, permits us, using the mathematical treatment, to measure very small phase variations. The article is organized as follows: in Sec. II we present the experimental setup. In Sec. III we present the Abel inversion method. The phase shift measurement method is presented in Sec. IV. The experimental results are in Sec. V. In Sec. VI gas jet characterizations are discussed, and we present a brief conclusion.

II. EXPERIMENTAL SETUP

The experiment was performed in the gas jet facility experimental room at LULI. The experimental configuration is shown in Fig. 1. A green He–Ne laser beam working at 532.5 nm is expanded and collimated to a 1 cm diam beam which propagates in the vacuum chamber. The Mach–Zehnder interferometer is located in the vacuum chamber. The beamsplitters and mirrors of the interferometer have a surface quality of $\lambda/20$. The gas jet is positioned in one arm of the Mach–Zehnder interferometer (see Fig. 1). Outside the vacuum chamber an $f/5$ spherical lens images the gas jet

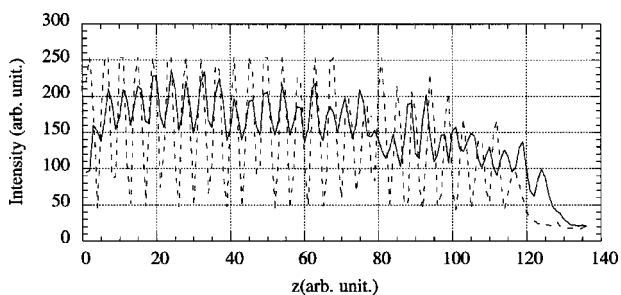


FIG. 3. Intensity profile in the fringe pattern: without gas (dashed line) and with gas (continuous line).

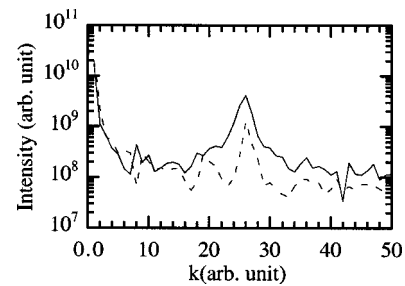


FIG. 4. k spectrum of the intensity profile: without gas (dashed line) and with gas (continuous line).

onto a linear charge coupled Device (CCD) detector. The image is demagnified (1:2) in order to have all of the gas jet in the recorded image. A special effort was made to reduce the noise in the interferograms due to mechanical motions (pump or gas valve opening). The spatial resolution is limited by the pixel size and is, with the current magnification, about 15 μm . The backing pressure in the gas reservoir is measured with a pressure transducer. The vacuum pressure (less than 10^{-2} mbar) in the chamber is measured with a baratron. A commercial solenoid valve (made by Parker-Lucifer) that is normally closed can be opened, giving the gas jet a constant flow for 80 ms.

The evolution of the gas flow is obtained using a 2 ms optical shutter, which can be opened at different time using a delay box (the rise and fall times of the gas flow are of the order of 15 ms). A narrow 10 nm bandwidth interference filter centered at 530 nm was used to reduce the noise level. The CCD is connected to a computer in order to record the 8 bit images. Mathematical extractions of the phase shift variation and the Abel inversion are made directly during the experiment. Very good shot to shot reproducibility of the gas flow was observed.

III. ABEL INVERSION

A large number of optical diagnostics are based on phase shift measurement. This phase is always proportional to the product of the index of refraction with the optical path length. More precisely, it is proportional to the integral of index of refraction along the path length. It is thus necessary to know the index of refraction everywhere in the medium. If the medium is cylindrically symmetrical, the situation is

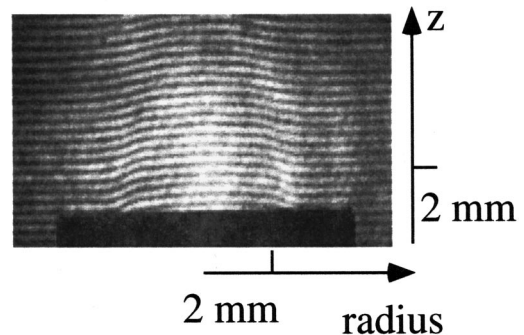


FIG. 5. Typical interferogram obtained with a Laval nozzle with 65 bar backing pressure.

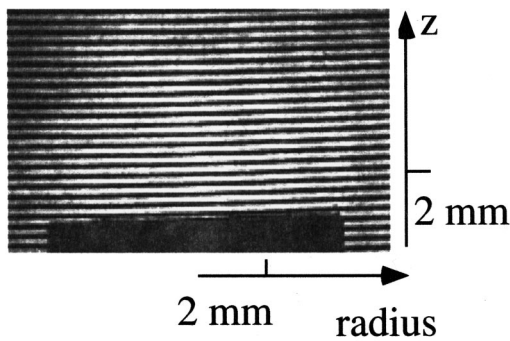


FIG. 6. Typical reference interferogram (i.e., without gas).

greatly simplified, and from the phase shift measurement along one direction we can deduce the radial distribution of the index of refraction. The transformation which permits an axial distribution to reach the radial one is called Abel inversion. In Fig. 2 we present a schematic of the phase shift along the y axis and its connection with the radial one.

The phase shift variation, integrated along the y axis, due to the optical path introduced by the gas jet is done by

$$\delta\varphi(x) = \frac{4\pi}{\lambda_0} \int_0^{y_0} [n(r) - 1] dy.$$

Changing the Cartesian coordinates by the cylindrical one, we obtain

$$\delta\varphi(x) = \frac{4\pi}{\lambda_0} \int_0^{r_0} \frac{[n(r) - 1] r dr}{(r^2 - x^2)^{1/2}}.$$

By using Abel's inversion this equation can be written as

$$\frac{4\pi[n(r) - 1]}{\lambda_0} = -\frac{1}{\pi} \int_r^{r_0} \frac{\varphi(x) dx}{(x^2 - r^2)^{1/2}}.$$

From the phase ϕ_k along the x -axis x for n equidistant values $x_k = kr_0/n$ (for $k=0, n-1$), we obtain the value of the index of refraction corresponding to $r_j = jr_0/n$ ($j=0, 1, 2, \dots, n-1$) from the simple relation

$$n_j - 1 = \frac{\lambda_0}{2\pi r_0} \sum_k a_{jk} \varphi_k,$$

where a_{jk} is the coefficient tabulated in Ref. 13.

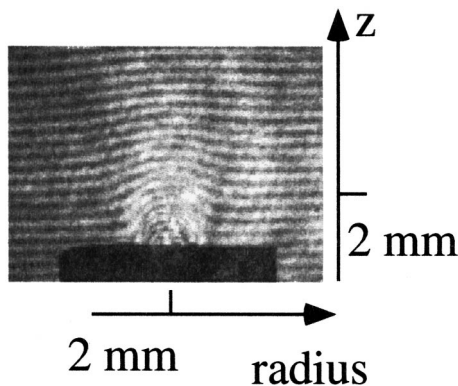


FIG. 7. Typical interferogram obtained with a cylindrical nozzle with 65 bar backing pressure.

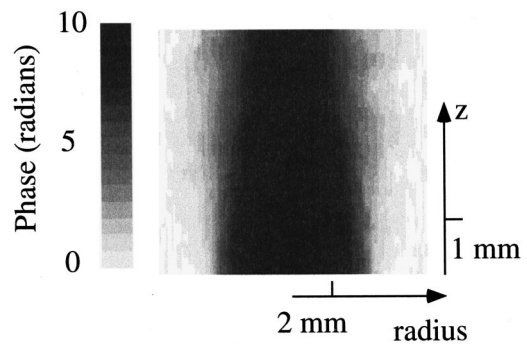


FIG. 8. Phase shift measurement obtained from the images in Figs. 5 and 6.

Finally the neutral gas density is then obtained by

$$N_k = (n_k - 1)N_0 / (n_{\text{gas}} - 1),$$

where n_{gas} is the index of refraction of the gas (for argon n is equal to 1.000 281) in the visible and N_0 the density of atoms at the standard temperature and pressure ($N_0 = 2.68 \times 10^{19} \text{ cm}^{-3}$).

IV. PHASE SHIFT MEASUREMENT METHOD

We now present the mathematical treatment^{14,15} used in order to get the phase shift from the interferogram images, one obtained with gas and the other one (the reference) obtained without gas. We first consider the intensity profile $I(z)$ along the z axis in the fringe pattern. In Fig. 3 we present the intensity profile obtained with and without gas. If the $\Phi(z)$ phase shift is induced by the gas, and there is d distance between two fringes, we have the following relation:

$$I(z) = 2I_0 \left[1 + \cos\left(\frac{2\pi z}{d} + \Phi(z)\right) \right].$$

If $\Phi(z)$ changes slowly over one fringe, the cosine factor corresponds to the fringe shift. The k spectrum presented in Fig. 4 is obtained by a Fourier transform of these plots. We see two components, one sharp at $k=0$ and a second one broader at $k=2\pi/d$. Phase information is deduced from the difference between the reference and the gas case at $k=2\pi/d$ as follows.

We take the inverse Fourier transform of these component in the gas case,

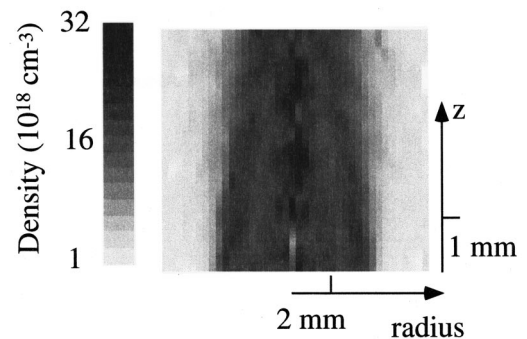


FIG. 9. Neutral density measurement obtained from the images in Figs. 5 and 6.

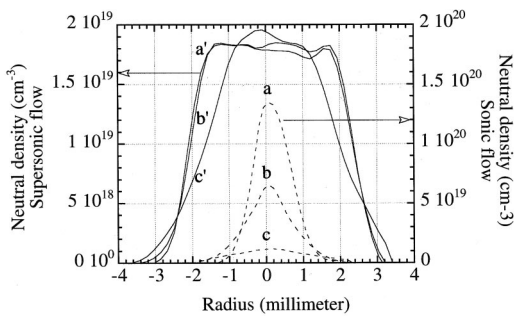


FIG. 10. Neutral density profile obtained with a Laval nozzle and a cylindrical nozzle, working with 65 bar backing pressure 0.5 (a), 1.5 (b), and 4 (c) mm from the nozzle.

$$I_g(z) = I_0 \exp[2i\pi z/d + i\Phi(z)],$$

and the inverse Fourier transform of these components in the reference case,

$$I_r(z) = I_0 \exp(2i\pi z/d),$$

then we deduce the phase from the logarithm of the ratio $I_g(z)/I_r(z)$. Comparing two reference images we deduce that this method allows us to measure a phase shift variation of the order of 0.05 rad.

V. EXPERIMENTAL RESULTS

A. Typical interferograms

We present in Fig. 5 an interferogram obtained with a Laval nozzle with argon gas at 65 bar (65 bar is the backing pressure, i.e., the pressure in the reservoir). The internal diameter at the output is 5 mm. The gas flow, ejected from the bottom to the top, is visible by the shift of the fringes. In Fig. 6 we present the corresponding reference interferogram. We can see the nozzle on the bottom. These data are recorded on a 378×286 pixel² CCD. The achieved spatial resolution of $15 \mu\text{m}$ is limited in our case by the pixel size. We present in Fig. 7 an interferogram obtained with a 1 mm diam sonic nozzle. We observe that with the supersonic jet, which is obtained using a Laval nozzle, the gas density stays constant along the flow axis z . In sonic expansion the neutral density decreases along this axis. This analysis will be detailed in Sec. VB.

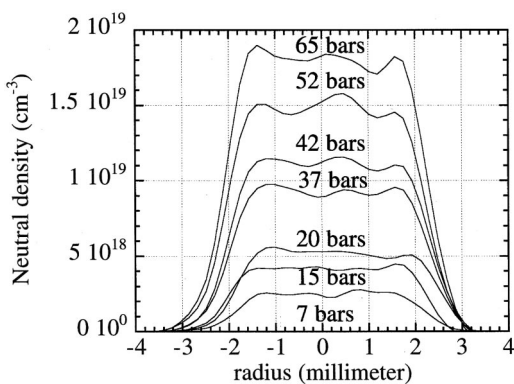


FIG. 11. Neutral density profile obtained with a Laval nozzle working with 65 bar backing pressure 1.5 mm from the nozzle.

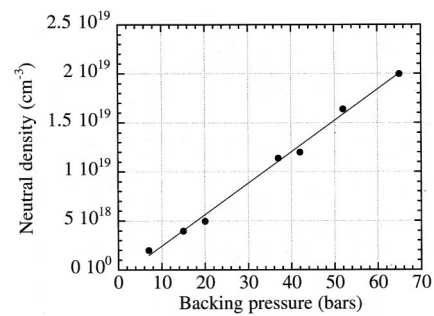


FIG. 12. Neutral density value as a function of the backing pressure.

B. Typical phase measurement

Using the mathematical treatment described in Sec. VA for each position along the z axis, we obtain from Figs. 5 and 6 the two-dimensional phase shift presented in Fig. 8. We observe that the phase profile is quite constant over a distance of several millimeters. The phase values change from 0 (at the gas jet edge) to a peak value of 10 rad. We also notice cylindrical symmetry, which allows us to use the Abel inversion technique.

C. Typical density measurement

In order to obtain a two-dimensional neutral density profile we made an Abel inversion for each line of the phase image. A two-dimensional neutral density profile, deduced from Fig. 8, is presented in Fig. 9. We observe that the gas density is quite constant over a distance of several millimeters. The gas density changes from 0 (at the gas jet edge) to a peak value of $2 \times 10^{19} \text{cm}^{-3}$. To define the symmetry axis we calculate for each z the integral of the phase along the radius. The symmetry axis is chosen when the integrals obtained from the left part ($r > 0$) and from the right part ($r < 0$) are equal.

VI. GAS JET CHARACTERIZATION

A. Neutral density profile for sonic and supersonic jets

The density profile is sensitive to the internal profile of the nozzle. For example, we present here the density profile obtained for a sonic and a supersonic jet. The sonic jet is realized using a cylindrical nozzle. In order to obtain supersonic flow a Laval nozzle is used. We observe in the first case (sonic one) that the neutral density profile is a parabolic function of the radius and that the on axis neutral density decreases exponentially with z , as $n(\text{cm}^{-3}) \approx 1.4 \times 10^{20} \times \exp[-0.64z(\text{mm})]$. In the supersonic case the on axis neutral density is constant over a distance of about 4 mm. The radial density profile presented in this case is a plateau. These results are shown in Fig. 10, in which we present the radial neutral density profile for the sonic and supersonic jet 0.5, 1.5, and 4 mm from the nozzle.

B. Neutral density versus the backing pressure

The radial neutral density profile is measured in a wide range of backing pressures from 5 to 65 bar. Even in the

lower backing pressure case the shape of these profiles is conserved. We present in Fig. 11 the radial density profiles for 5, 15, 25, 35, 42, 52, and 62 bar. It is interesting to note that the value of the density is a linear function (in this range of pressure) of the backing pressure. This result is shown in Fig. 12.

ACKNOWLEDGMENT

The gas jet facility experimental room is a new experimental area allocated for the study and the gas jet characterization. This facility is a specific undertaking of both the LOA (Laboratoire d'Optique Appliquée) and the LULI laboratories.

¹A. Modena *et al.*, *Nature (London), Phys. Sci.* **377**, 606 (1995).

²C. A. Coverdale, C. B. Darrow, C. D. Decker, W. B. Mori, K. C. Teng, K.

A. Marsh, C. E. Clayton, and C. Joshi, *Phys. Rev. Lett.* **74**, 23 (1995).

³J. Denavit and D. W. Phillion, *Phys. Plasmas* **1**, 1971 (1994).

⁴S. D. Baton *et al.*, *Phys. Rev. E* **57**, 5 (1998).

⁵H. Fiedorowicz, A. Bartnik, Z. Patron, and P. Parys, *Appl. Phys. Lett.* **62**, 2778 (1994).

⁶E. Fill, S. Borgstrom, J. Larson, T. Starczewski, and C. G. Svanberg, *Phys. Rev. E* **51**, 6016 (1995).

⁷V. Malka *et al.*, *Phys. Rev. Lett.* **16**, 2979 (1997).

⁸K. Krushelnick, A. Ting, C. I. Moore, H. R. Burris, E. Esarey, P. Sprangle, and M. Baine, *Phys. Rev. Lett.* **78**, 21 (1997).

⁹S. P. Nikitin, T. M. Antonsen, T. R. Clark, Yuelin Li, and H. M. Milchberg, *Opt. Lett.* **22**, 23 (1997).

¹⁰Y. M. Li and R. Fedosejevs, *Meas. Sci. Technol.* **5**, 1197 (1994).

¹¹A. Behjat, G. J. Tallents, and D. Neely, *J. Phys. D: Appl. Phys.* **30**, 2872 (1997).

¹²J. Winckler, *Rev. Sci. Instrum.* **19**, 307 (1948).

¹³K. Bockasten, *J. Opt. Soc. Am.* **51**, 943 (1961).

¹⁴J. P. Geindre, P. Audebert, S. Rebibo, and J. C. Gauthier, *LULI Annual Report*, 1998, p. 127.

¹⁵K. A. Nugent, *Appl. Opt.* **18**, 3101 (1985).